Nanoporous Carbon Allotropes by Septupling Map Operations

Mircea V. Diudea

Faculty of Chemistry and Chemical Engineering, Babes-Bolyai University, 400028 Cluj, Romania

Received February 14, 2005

Spongy carbon nanostructures, also called schwarzites, have been synthesized. They consist of highly connected covalent networks, periodic in the three dimensions of Euclidean space. The intimate structure of schwarzites has a topology of triply periodic minimal surfaces. They can be tessellated by some geometric operations on maps, including the newly proposed septupling operations. Formulas for calculating the lattice parameters of iteratively transformed maps are presented. Examples are given for both finite/closed cages and infinite/open all-sp^2 carbon structures. Strain energy calculations for structures, consisting of thousands of atoms, show that such carbon allotropes are very relaxed and approach to the non-strained graphite sheet.

1. INTRODUCTION

Covering a local planar surface by various polygonal or curved regions is an ancient human activity. It occurred in house building, particularly in floor, window, and ceiling decoration. There were three well-known regular Platonic tessellations (i.e., coverings by a single face type and a single vertex degree): (4, 4), (6, 3), and (3, 6). The Greek and Roman mosaics were very appreciated in this respect.

Covering is nowadays a mathematically founded science.[1] It makes use of the graph and set theory and often gets inspiration from art and architecture.

Covering transformation is one of the ways that the chemical reactions occurring in nanostructures can be understood.[2−4]

Among the carbon allotropes, intensively studied in the past decade,[5−9] the only orientable closed surface (S) entirely coverable by a benzenoid lattice is the torus. A polyhedral cage obeys the Euler theorem:[10]

$$v - e + f = \chi(S) = 2(1 - g) \tag{1}$$

where $\chi(S)$ is the Euler characteristic ($\chi(S) = 2-2g$) and v, e, f, and g are, respectively, the number of vertices, edges, faces, and genus—zero for the sphere and unity in case of the torus.

Spongy carbon nanostructures, also called schwarzites, have been synthesized.[11−13] The low density materials consist of highly connected sp^2 carbon covalent networks, periodic in the three dimensions of Euclidean space. The intimate structure of schwarzites has a topology of triply periodic minimal surfaces (TPMSs). They appear to result by the self-assembly of various repeat units, some of them encountered in the 3D junctions of nanotubes.

These negatively curved surfaces can be variously tessellated by using some map operations, two twin septupling-open operations that introduce heptagons within a polyhedral lattice as elements of negative curvature being of crucial importance (see the next section).

This paper is organized as follows. The second section defines the septupling map operations and their transformed lattice parameters. The third section deals with the molecular realization of the two operations, both as closed and open structures. The last two sections provide conclusions and references.

2. SEPTUPLING OPERATIONS ON MAPS

A map (M) is a combinatorial representation of a closed surface.[14,15] Two main operations on maps, leading to Platonic tessellations, are known: the septupling S_1 and S_2 operations.[16,17]

The S_1 operation was also called[16] the Capra (Ca) operation. It is a composite operation that can be written as a sequence of simple operations:

$$S_1(M) = Tr_{P_5}(P_5(M)] \tag{2}$$

with Tr_{P_5} representing the truncation of new, face centered vertices introduced by P_5 pentagonal capping, which involves an E_2 (i.e., two new points put on each edge) operation.

Recall that P_5 is a particular case of the *polygonal capping* ($P_{s;}$ $s = 3, 4, 5$), realizable[17,18] by the following steps: (i) add a new vertex in the center of a face, (ii) put $s - 3$ points on the boundary edges, and (iii) connect the central point with one vertex (the end points included) on each edge. In this way, the parent face is covered by trigons ($s = 3$), tetragons ($s = 4$), and pentagons ($s = 5$).

The nuclearity of the Goldberg[19] polyhedra (related to the fullerenes) is obtained by using the parameters

$$m = (a^2 + ab + b^2);\ a \geq b;\ a + b > 0 \tag{3}$$

which is the multiplication factor $m = v/v_0$ in a three-valent map transformed by a given operation. The m factor has been used since ancient Egyptian times for calculating the volume of truncated pyramid, of height h: $V = mh/3$. S_1 corresponds to $m(a, b) = m(2, 1) = 7$.

S_1 insulates any face of M with its own hexagons, which are not shared with any other face. It is an intrinsic chiral operation (it rotates the parent edges by $\pi/(3/2)s$) and was extensively illustrated in refs 17 and 18. Because pentangulation of a face can be done either clockwise or counterclockwise, it results in an enantiomeric pair of objects:

10.1021/ci050054y CCC: $30.25
Published on Web 05/14/2005

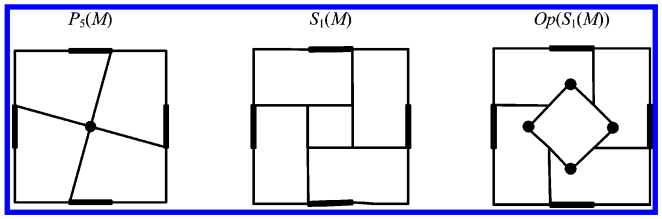

Figure 1. Septupling S_1 operation on a square face, up to the open structure.

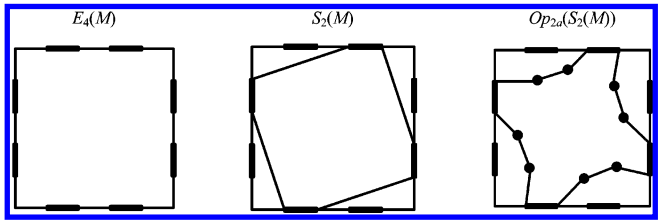

Figure 2. Septupling S_2 operation on a square face, up to the open structure.

$S_{1S}(M)$ and $S_{1R}(M)$, with the subscript *S* and *R* given in terms of the *sinister*/*rectus* stereochemical isomery.[16]

S_1 can continue with the "open" operation

$$Op_r(S_i(M)) \tag{4}$$

where *r* represents the number of points added on the boundary of the parent faces, which become the "open" faces. The resulting open objects have all the polygons of the same $(6 + r)$ size. The above operation sequence enables the construction of negatively curved networks (see below). Figure 1 gives the steps of S_1 realization on a square face in a trivalent lattice, up to the open structure.

The transformed lattice parameters are shown in the following relations:

$$S_1(M) \text{ and } S_2(M): \quad v = v_0(2d_0 + 1);\ e = 7e_0;\ f = f_0(s_0 + 1) \tag{5}$$

$$Op(S_1(M)): \quad v_{Op} = v_0(3d_0 + 1);\ e_{Op} = 9e_0;\ f_{Op} = f_0 s_0 \tag{6}$$

$$Op_{2a}(S_2(M)): \quad v_{Op} = (4d_0 + 1)v_0;\ e_{Op} = 11e_0;\ f_{Op} = f_0 s_0 \tag{7}$$

where *d* and *s* are the vertex degree and face size, respectively; the subscript zero refers to the original map *M*.

The S_2 operation[17,20] is a simpler one (Figure 2); it can be achieved by putting four vertices on each edge of the parent map *M* (E_4 operation) and, next, joining these new vertices in order $(-1, +3)$:

$$S_2 = J_{(-1,+3)}(E_4(M)) \tag{8}$$

It insulates the double-sized parent faces by pentagons and the parent vertices by pentagon d_0 multiples; the transformed objects are nonchiral ones.

However, chirality is brought by the *Op* operation Op_{2a}, achieved by putting two points on alternative edges of the double-sized parent face boundary (Figure 2). In the case of a closed product, the transformed lattice parameters are identical to those of S_1 (eq 5); differences appear in cases of open objects (eqs 6 and 7). Note that both the septupling operations keep the parent vertices (see the vertex counting formulas, eq 5).

The iterative *n*-time application (on maps with any vertex degree, $d_0 \geq 3$) leads to the following lattice parameters, transformed by both S_1 and S_2:

$$v_n = v_0 q_n$$
$$e_n = e_0 m^n$$
$$f_n = f_0(s_0 p_n + 1) \tag{9}$$

where

$$q_n = 2d_0 p_n + 1;\ n \geq 2 \tag{10}$$

$$p_n = \sum_{i=0}^{n-1} m^i = (m^n - 1)/(m - 1) = m(m...(m + 1)... + 1)_{n-2} + 1 \tag{11}$$

The parameter *m* is that defined in relation 3. From eq 10, it is obvious that

$$p_n = (q_n - 1)/2d_0 \tag{12}$$

For trivalent maps (i.e., those with $d_0 = 3$), the above parameters become

$$q_n = m^n \tag{13}$$

$$p_n = (m^n - 1)/6 \tag{14}$$

$$v_n = v_0 m^n$$
$$e_n = e_0 m^n$$
$$f_n = f_0(s_0(m^n - 1)/6 + 1) \tag{15}$$

In the case of a cage opening after the n^{th} iteration, the lattice parameters are as follows:

$$v_{n,Op}(S_1) = v_0 q_n + f_0 s_0 = v_0(d_0 + q_n)$$
$$e_{n,Op}(S_1) = e_0 m^n + f_0 s_0 = e_0(m^n + 2)$$
$$f_{n,Op}(S_1) = f_0(s_0 p_n + 1) - f_0 = f_0 s_0 p_n \tag{16}$$

$$v_{n,Op_{2a}}(S_2) = v_0 q_n + 2f_0 s_0 = v_0(2d_0 + q_n)$$
$$e_{n,Op_{2a}}(S_2) = e_0 m^n + 2f_0 s_0 = e_0(m^n + 4)$$
$$f_{n,Op_{2a}}(S_2) = f_0(s_0 p_n + 1) - f_0 = f_0 s_0 p_n \tag{17}$$

The two septupling operations represent twin operations, in that the transformed objects, representing repeat units in D- and P-type negatively curved surfaces, belong to the complementary labyrinths (see the next section).

3. MOLECULAR REALIZATION

The sequence of different operations (the open ones included) enables the construction of various objects, with both positive and negative curvature.[16,21−24]

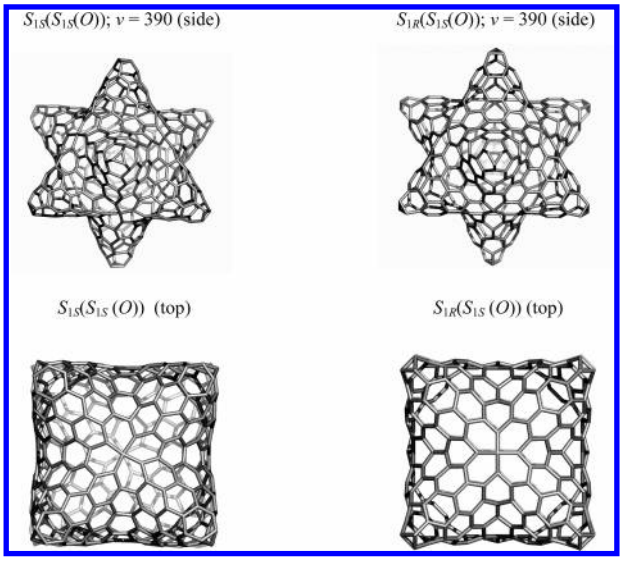

Figure 3. Sequence of S_1 prochiral operations on the octahedron; the S_{1S}, S_{1S} transform is still twisted, whereas the S_{1R}, S_{1S} one is no longer chiral.

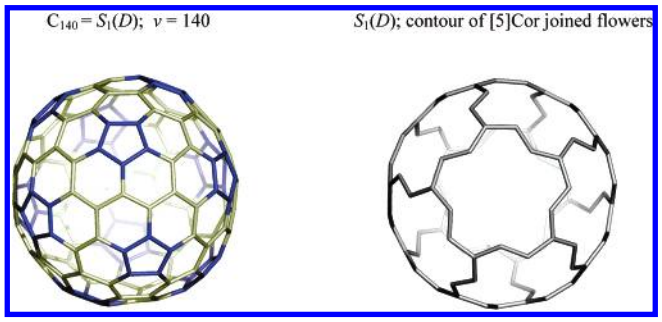

Figure 4. Chiral fullerene C_{140} and its Platonic covering (([5]Cor)3).

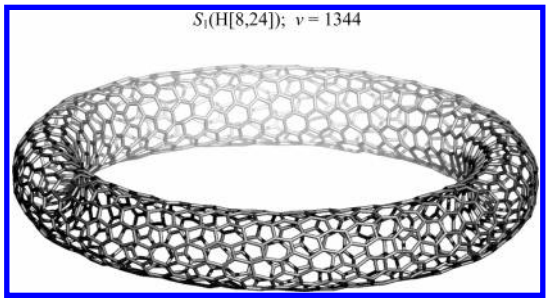

Figure 5. Chiral toroidal structure with the Platonic covering (([6]Cor)3).

3.1. Closed Objects. As mentioned above, S_1 rotates the parent bonds, so that it provides chiral transforms. The iterative application of S_1 may lead to either chiral/twisted or nonchiral/nontwisted transforms; for example, the sequence $S_{1S}(S_{1S}(M))$ results in a twisted structure while $S_{1R}(S_{1S}(M))$ provides a nontwisted object (Figure 3).

When applied on fullerenes, S_1 leads to chiral structures. In this respect, C_{140} is the only fullerene with a Platonic covering (a single size of equivalent faces) of the form (([5]Cor)3), where [5]Cor is the [5]corannulenic "supra face"[17,18] (Figure 4). In other fullerenes, S_1 provides Archimedean coverings (([5]Cor,[6]Cor)3).

Applied on polyhex toroidal objects, S_1 provides the Platonic (([6]Cor)3) covering (Figure 5).

In the opposite, S_2 leads to non-twisted objects when applied to closed cages. Its iterative application reveals the fractal fashion of the covering (Figure 6). The fractal characteristic[25,26] can be seen even in the algebraic form of the p_n parameter (eq 11).

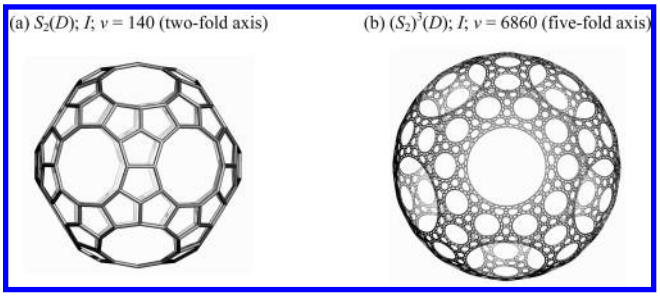

Figure 6. Iterative S_2 operation on the dodecahedron; observe the fractal covering in case of three-time repetition (b).

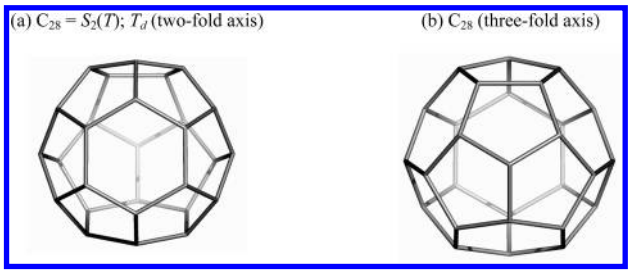

Figure 7. C_{28}—the only fullerene constructible by S_2.

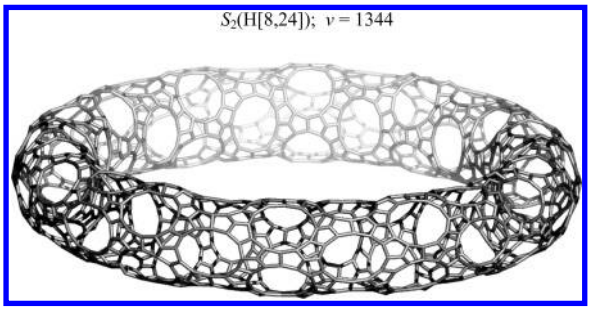

Figure 8. Toroidal lattice having Archimedean covering ((5, 12)3) $= S_2(6, 3)$, with local signature (3, 0).

The only fullerene constructible by S_2 is C_{28}, when applied on the tetrahedron (Figure 7).

Applied on toroidal objects, S_2 leads to an Archimedean covering (Figure 8). All of the above closed objects show a positive curvature (i.e., they have $\chi \geq 0$, see eq 1).

3.2. Open Objects. The negative curvature can be induced in graphite (the reference, of zero curvature) by replacing hexagons with heptagons, or larger sized rings. Such nets form only open structures, in contrast to those derived by introducing pentagons or smaller rings (which bring a positive curvature) that form closed cages/polyhedra (see Section 3.1).

Recall that an orientable surface S (i.e., having two sides) is characterized by the Euler parameter $\chi(S) = 2(1 - g)$ (see eq 1). $\chi(S)$ is directly calculable by the genus g, which is the number of holes required by a plastic sphere to make it homeomorphic to S. Positive/negative χ values indicate positive/negative curvatures of a lattice (M) embedded in S. An embedding is a representation of a graph on a closed surface such that no crossing lines appear.[27,28]

Curvature is the amount by which a geometric object deviates from being *flat*. It is usually measured either as Gaussian curvature (K) or as a mean curvature (H). These are defined at each point on the surface as functions of the

surface principal curvatures at that point as follows:

$$K = \pm k_1 k_2 \tag{18}$$

$$H = \frac{1}{2}(k_1 + k_2) \tag{19}$$

To evaluate these at a given point of the surface, consider the intersection of the surface with a plane containing a fixed normal vector at the point. This intersection is a plane curve, having a curvature $k = 1/r$; if the plane is varied, this curvature will change, and there are two extreme values, the maximal and the minimal curvature, called the *principal curvatures*, k_1 and k_2. Accordingly, the extreme directions are called principal directions. Usually, a curvature is taken to be positive if the curve turns in the same direction as the surface's chosen normal, otherwise it is negative.[2,20,29] A surface (S) is *flat* if $K(p) = 0$, and it is *minimal* if $H(p) = 0$, for every $p \in S$.

The integral of the Gaussian curvature over the whole surface is closely related to the surface's Euler characteristic $\chi(S)$ (*Gauss−Bonnet* theorem):[2,29]

$$\int_S K dS = 2\pi\chi(S) \tag{20}$$

The above theorem relates the geometric curvature to the topology (see eq 1).

If S is a topohedral surface in 3D, then the overall angular defects (i.e., disclinations) are proportional to the Euler characteristic (Descartes' theorem):[2,29]

$$\sum_p^S \phi_p = 2\pi\chi(S) \tag{21}$$

Mean curvature is closely related to the first variation of surface area. Surfaces having a mean curvature $H = 0$, everywhere, are *minimal surfaces* (with minimal local area). The shapes taken by soap films are minimal surfaces. Unlike Gaussian curvature, the mean curvature depends on the embedding; for instance, a cylinder and a plane are locally isometric, but the mean curvature of a plane is zero and that of a cylinder is nonzero.

The intimate structure of spongy carbon allotropes is that of an infinite TPMS, of negative curvature. Such a surface is saddle-shaped everywhere except at certain *flat points*.

If a TPMS has no self-intersections, it partitions the space into two disjoint labyrinthine regions. Its topology is characterized by two interpenetrating networks, the *labyrinth graphs*.[30]

Our goal is to generate various repeat units useful for building up some infinite/open lattices. The operation leading to open (repeat) units is Op_r (eq 4), which is an E_r homeomorphic transformation of the parent edges. Most often, $r = 1$; thus, it is omitted. It can be associated with any composite operation.

Keeping in mind eqs 6 and 7, the genus of an open object $Op(M)$ is calculable as[16]

$$\chi(Op(M)) = v_{Op} - e_{Op} + f_{Op} = v_0 - e_0 = 2 - 2g \tag{22}$$

$$g = (2 - v_0 + e_0)/2 = f_0/2 \tag{23}$$

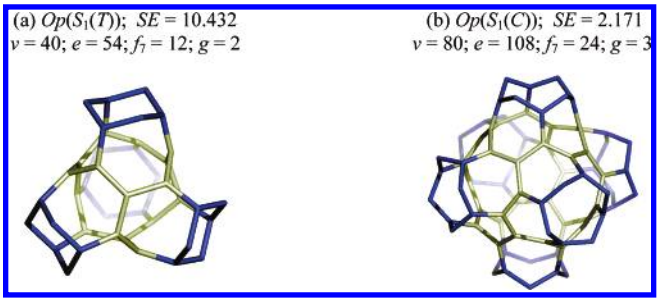

Figure 9. Opening (*Op*) operation leads to negative curvature lattices, embedded as repeat units in surfaces of genus (a) 2 and (b) 3.

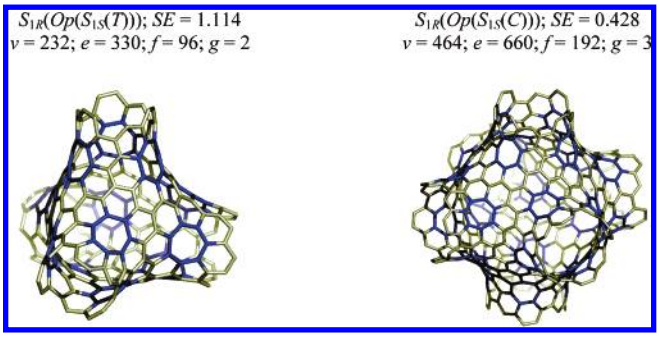

Figure 10. Units of negative curvature, derived by iterative septupling of a tetrahedron and a cube.

Relation 23 comes from the spherical character of the parent polyhedron, for which the Euler relation is written as $v_0 - e_0 + f_0 = 2$. Because f_0 is just the number of open faces, relation 23 can be extended to any open object, eventually derived from a spherical polyhedron by a composite operation.

Clearly, lattices with $g > 1$ will have a negative $\chi(Op(M))$ and, consequently, a negative curvature. For the five platonic solids, the genus of the corresponding $Op(M)$ are 2 (tetrahedron, T), 3 (cube, C), 4 (octahedron, O), 6 (dodecahedron, D), and 10 (icosahedron, I).

Note that $Op(S_1(M))$ provides an all-heptagon Platonic (7, 3) covering of the negatively curved units derived from the Platonic solids. Figure 9 illustrates the $Op(S_1(M))$ realization.

Iterative *septupling* of open objects leads to more relaxed units, as apparent when comparing the strain energy (SE) per sp^2 atom (in kcal/mol, in terms of the POAV1 theory),[31−34] given in the tops of Figures 9 and 10. Such units can be viewed as rational models for the 3D junctions of nanotubes.[20,21]

The same Platonic (7, 3) covering is obtained by S_2, when followed by the *Op* operation, which can be performed in various modes, two of the most useful being illustrated in Figure 11. Observe that the object in Figure 11a fits to a "zigzag" nanotube, whereas that in Figure 11b fits to an "armchair" one. In the *Op* operation, the subscript 11 means one new point on each edge, whereas 2a means two new points put on alternative edges of a boundary in which folding is twice that of the parent faces.

3.2.1. D- and FRD-Type Schwarzites. A spongy carbon allotrope, with all covalently bonded sp^2 atoms, whose lattice can be embedded in a TPMS is called a TPMS graphene or a *periodic schwarzite*,[11,35−37] in the honor of H. A. Schwarz,[38,39] who first investigated, in the early nineteenth century, the differential geometry of such surfaces. The most frequently

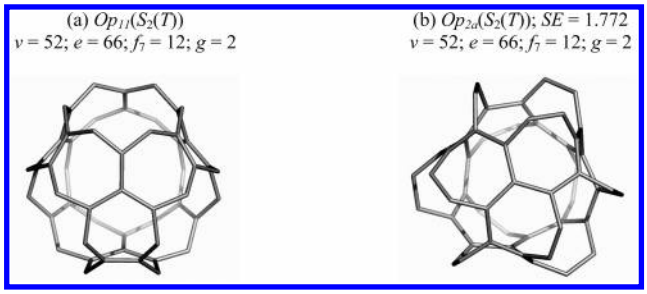

Figure 11. Opening (*Op*) operation leads to negative curvature lattices, embedded as repeat units in surfaces of genus 2.

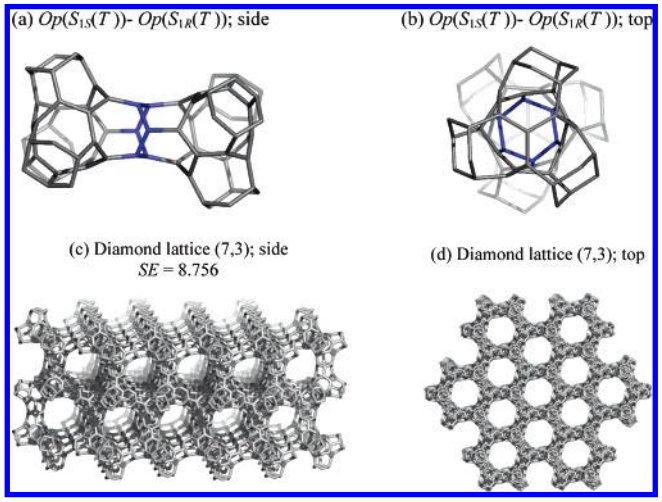

Figure 12. Repeated units and the sp^2 diamond (D-type surface) of Platonic (7, 3) tessellation.

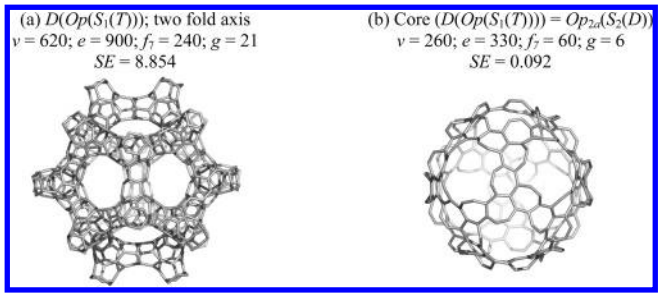

Figure 13. Supra-*D* structure of (7, 3) Platonic tessellation, by S_1, and its core.

considered minimal surfaces in modeling schwarzites are of D, FRD, and P types.[11,13,22−24,35−37,40−42]

Various repeat units of the D schwarzites can be designed by applying the septupling operations S_1 and S_2. Parts a and b of Figure 12 illustrate the chiral pair of the S_1-transformed tetrahedron, $Op(S_{1S}(T))$ and $Op(S_{1R}(T))$, put together by identifying the open face between the two structures, such as they appear (in an "intercalate" conformation) in the bi-elemental cell of an sp^2 diamond lattice, having a (7, 3) Platonic tessellation (Figure 12c,d). For diamond-like structures, supplementary information can be found in refs 35 and 36.

The building block $Op(S_1(T))$ (Figure 9a), as an "eclipsed" bi-elemental cell, enabled the construction of a supradodecahedron,[17,18] a multitorus of genus 21, having a (7, 3) Platonic tessellation (Figure 13a).

Its core is given by $Op_{2a}(S_2(D))$ (Figure 13b). A similar structure can be built starting from $Op_{2a}(S_2(T))$ (Figure 11b), whereas its core is $Op(S_1(D))$ (Figure 14a,b). Such supra-

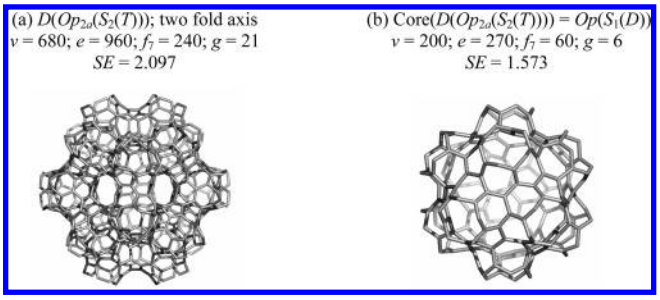

Figure 14. Supra-*D* structure of (7, 3) Platonic tessellation, by S_2, and its core.

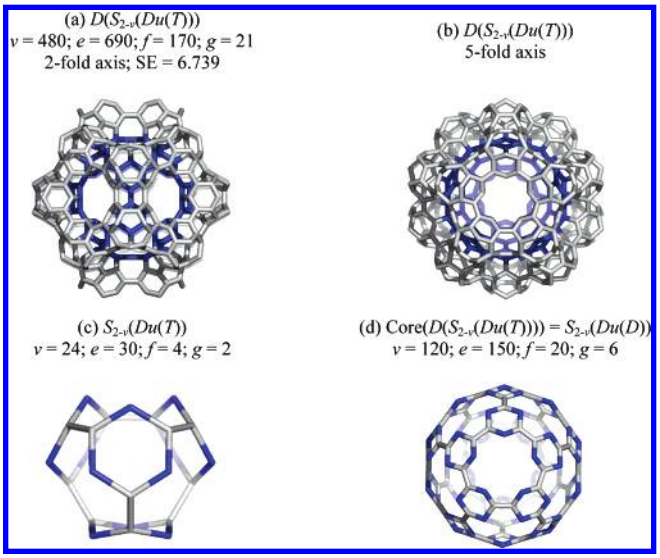

Figure 15. Supra-*D*, as one of the twin labyrinths of the FRD-type surface, built up from either $S_{2-v}(Du(T))$ or $S_{2-v}(Du(D))$ units.

dodecahedra represent one of the twin labyrinths interlaced in the construction of the FRD-type surface; they could appear by a self-assembling process, as shown in ref 20. Thus, the unit graphs of the twin labyrinths can be written as $Op(S_1(T))/Op_{2a}(S_2(D))$ and $Op_{2a}(S_2(T))/Op(S_1(D))$, respectively. The free boundary changes from "zigzag" (S_1) to "armchair" (S_2) and vice-versa. This is just the expected complementarity of the objects derived by the twin septupling open operations.

Note that cages of genus 11 (as obtained by capping the above supradodecahedra) have been previously proposed by Terrones and Terrones.[43]

A simpler realization is illustrated in Figure 15. The supradodecahedron (Figure 15a,b) is built up on the repeat unit C_{24} (Figure 15c), derived as $S_{2-v}(Du(T))$, with $-v$ denoting the deletion of all vertices belonging to the dual of the parent map, following S_2. The object $S_{2-v}(Du(D))$ (Figure 15d) is its core complement in the dual labyrinth lattice. The units $S_{2-v}(Du(T))/S_{2-v}(Du(D))$ provide an FRD-type surface[40] (space group F_d3m; unit cell of tetrahedral symmetry).

Connecting $S_{2-v}(Du(D))$ to the other twelve identical objects results in an FRD domain of genus 66 (Figure 16a). It can be capped to obtain the compact array of 13 spherical domains[20] (Figure 16c,d). The above array shows a core identical to the supradodecahedron $D(S_{2-v}(Du(T)))$ (Figure 15a,b). This clearly demonstrates the complementarity of the units derived by the same operation sequence from tetrahedra and dodecahedra, respectively, concerted in the construction of FRD-type surfaces.

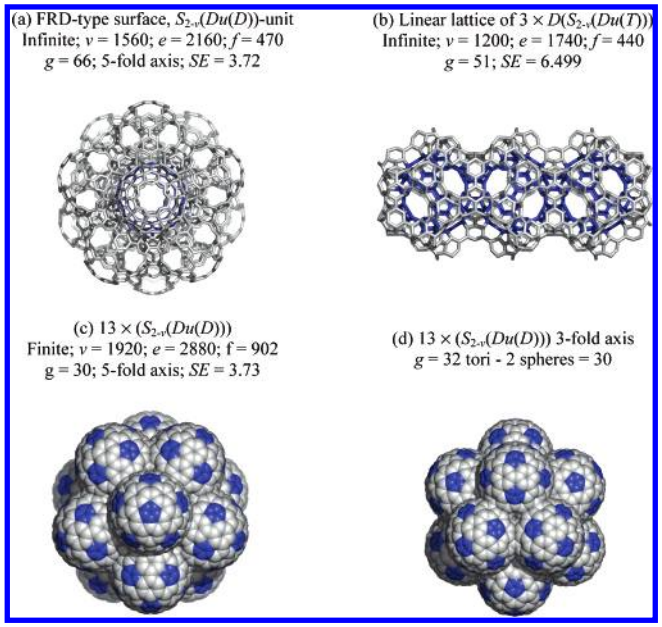

Figure 16. Spherical (a, c, d) and linear (b) evolution of the structures in Figure 15.

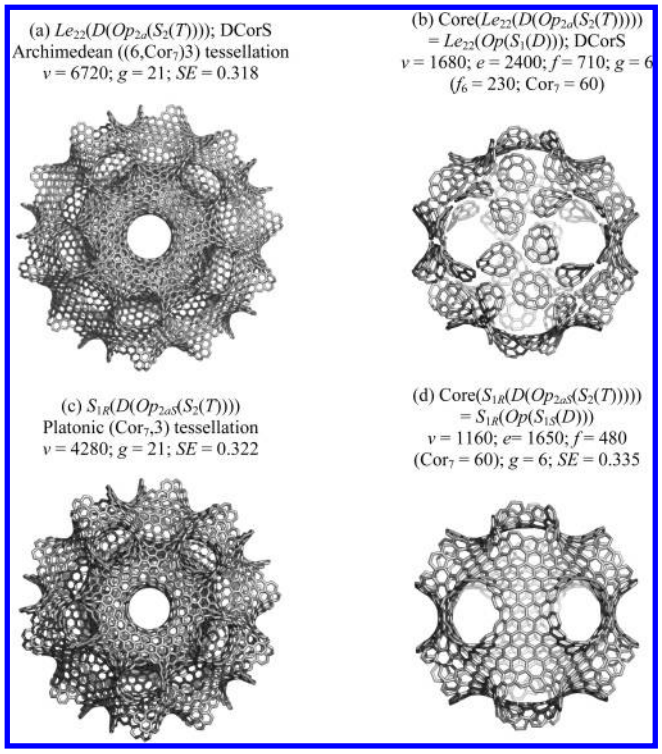

Figure 17. Supra-*D* (S_2-started) structure (Figure 14a) transformed by Le_{22} and S_1 operations.

The unit $D(S_{2-v}(Du(T)))$ may also evolve in a linear array, as shown in Figure 16b.

The supra-*D* (S_2-started) structure (Figure 14a) can be further transformed in view of obtaining different Platonic or Archimedean tessellations, as shown in Figure 17.

The object transformed by Le_{22} operations,[44] with *T*/*D* dual lattice units $Le_{22}(Op_{2a}(S_2(T)))/Le_{22}(Op(S_1(D)))$, shows a disjoint corannulenic[17,18] structure (DCorS; Figure 17a,b). Its covering is an Archimedean ((6, [7]Cor)3), supplementary information being given in the tops of the figures.

Next, the S_1 operation provides a Platonic covering of joined [7]Cor supra faces (Figure 17c,d). The dual lattice

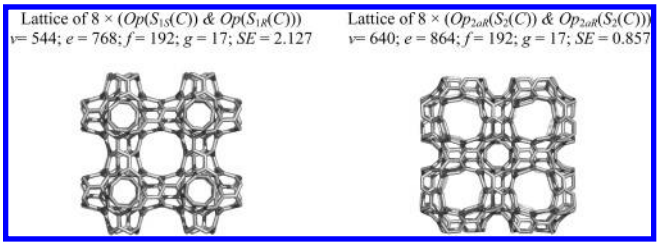

Figure 18. Platonic (7, 3) tessellation of the P-type surface by the two septupling map operations.

units are $S_{1R}(Op_{2aS}(S_2(T)))/S_{1R}(Op(S_{1S}(D)))$. The same complementarity of the twin septupling operations is observed.

It is known that the curvature elastic[36] energy decreases in the series: sphere > cylinder > saddle > flat surface. The average SE values for C_{60} and a (6, 6) nanotube are about 8.3 and 1.6 kcal/mol, respectively. In the open units of infinite lattices herein designed, the strain ranges between 0.31 and 0.85 (see the tops of the figures), clearly supporting the above energy decreasing sequence. Clearly, as the number of atoms increases, the lattice becomes more and more relaxed. Thus, the energy gain from the repeat units to large structures will promote the self-assembling reaction.

Corannulenic (DCorS) coverings are expected to give a particular magnetic response, as a result of the diamagnetic ring current of the flower periphery (see also ref 45).

At this stage of the discussion, recall that among several proposed synthetic routes for carbon schwarzites, two of them appear to be conceivable: one suggests the carbonization of foamed polymers, whereas the other infers the fullerenes as templates. Both routes ultimately converge to the dual labyrinth structures, which could evolve from either a tetrahedral or a spherical (dodecahedral) repeat unit.

3.2.2. P-Type Schwarzites. The P-type surface has the space group P_n3m; molecular realization is mainly achieved by the two septupling map operations (Figure 18). Observe the combination of the prochiral units, provided by these operations, in obtaining nontwisted (achiral) lattices of a high genus. The dual lattice units are easily deduced as $Op(S_1(C))/Op_{2a}(S_2(C))$, disregarding the chirality. Lattices of this type have been described in refs 20−24, 41, and 42.

The sequence $S_i(Op_n(S_i(M)))$ or other similar ones may provide variations of the P-surface covering (e.g., those shown in Figure 19).

Note that (7,3) tessellation is also called Klein tessellation, after F. Klein,[46,47] whose graph is a representation of the automorphism of the (heptakis) octahedral group.[48]

The large hollows appearing in the above objects could explain the porosity of the spongy carbon materials. Unit blocks provided by $Op(S_1(C))$ (Figure 18) could model the junctions of carbon nanotubes, obtainable by "nano-welding" crossing tubes in an electron beam.[49]

All of the presented structures have been computed by the original software program CageVersatile 1.5.[50]

CONCLUSIONS

Spongy carbon nanostructures, also called schwarzites, which have been recently synthesized, consist of highly connected covalent networks, periodic in the three dimensions of Euclidean space. TPMSs were claimed as the intimate structure of schwarzites.

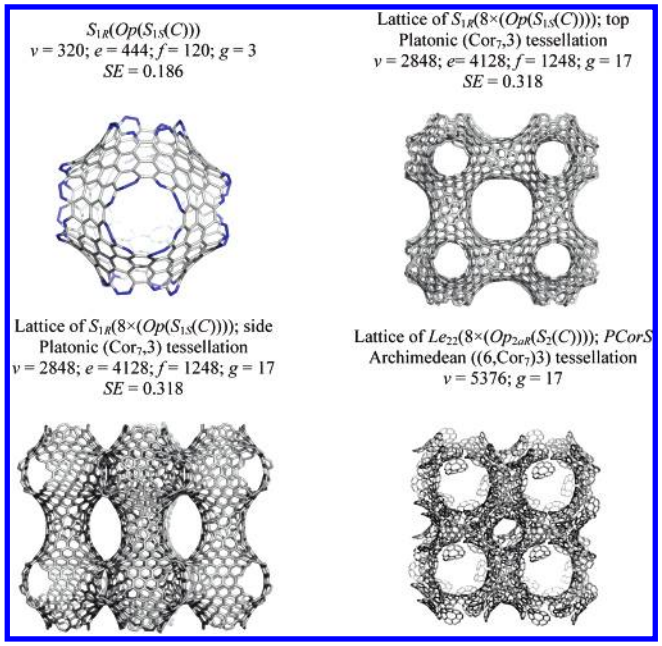

Figure 19. Transformed $S_1(M)$ covering of the P-type surface.

Such networks, of high genus, can be tessellated by some geometric operations on maps, including the newly proposed septupling operations. Formulas for calculating the lattice parameters of iteratively transformed maps were given.

POAV1 (POAV = π-orbital axis vector) strain energy calculations for the structures, including thousands of atoms, have shown that such structures are very relaxed and approach a graphite sheet in structure. Data support previous literature results indicating a decrease of energy in the series: sphere > cylinder > saddle > flat surface.

Examples, given for both finite/closed cages and infinite/open all-sp^2 carbon structures, prove the usefulness of the two septupling operations in the design of various structural units that, eventually, could self-organize in nanoporous materials.

REFERENCES AND NOTES

(1) Grünbaum, B.; Shephard, G. C. *Tilings and Patterns*; Freeman: New York, 1985.

(2) Klein, D. J.; Zhu, H. All-conjugated carbon species. In *From Chemical Topology to Three-Dimensional Geometry*; Balaban, A. T., Ed.; Plenum Press: New York, 1997; pp 297−341.

(3) de La Vaissière, B.; Fowler, P. W.; Deza, M. Codes in Platonic, Archimedean, Catalan, and related polyhedra: a model for maximum addition patterns in chemical cages. *J. Chem. Inf. Comput. Sci.* **2001**, *41*, 376−386.

(4) Deza, M.; Fowler, P. W.; Shtorgin, M.; Vietze, K. Pentaheptite modifications of the graphite sheet. *J. Chem. Inf. Comput. Sci.* **2000**, *40*, 1325−1332.

(5) Endo, M.; Iijima, S.; Dresselhaus, M. S. *Carbon Nanotubes*; Pergamon Press: Elmsford, NY, 1996.

(6) Fowler, P. W.; Manolopolous, D. E. *An atlas of fullerenes*; Oxford University Press: London, 1994.

(7) Dresselhaus, M. S.; Dresselhaus, G.; Eklund, P. C. *Science of fullerenes and carbon nanotubes*; Academic Press: San Diego, 1996.

(8) Tanaka, K.; Yamabe, T.; Fukui, K. *The science and technology of carbon nanotubes*; Elsevier: New York, 1999.

(9) *From Chemical Topology to three-dimensional Geometry*; Balaban, A. T., Ed.; Plenum Press: New York, 1997.

(10) Euler, L. Elementa doctrinae solidorum. *Novi Comment. Acad. Sci. I. Petropolitanae* **1758**, *4*, 109−160.

(11) Benedek, G.; Vahedi-Tafreshi, H.; Barborini, E.; Piseri, P.; Milani, P.; Ducati, C.; Robertson, J. The structure of negatively curved spongy carbon. *Diamond Relat. Mater.* **2003**, *12*, 768−773.

(12) Zaakhidov, A. A.; Baughman, R. H.; Iqbal, Z.; Cui, C.; Khayrullin, I.; Santas, S. O.; Marti, J.; Ralchenko, V. G. Carbon structures with three-dimensional periodicity at optical wavelengths. *Science* **1998**, *282*, 5390.

(13) Barborini, E.; Piseri, P.; Milani, P.; Benedek, G.; Ducati, C.; Robertson, J. Negatively curved spongy carbon. *Appl. Phys. Lett.* **2002**, *81*, 3359−3361.

(14) Pisanski, T.; Randić, M. Bridges between geometry and graph theory. In *Geometry at work: a collection of papers showing applications of Geometry;* Gorini, C. A., Ed.; Mathematical Association of America: Washington, DC, 2000; Vol. 53, p 174−194.

(15) Fowler, P. W.; Pisanski, T. Leapfrog transformations and polyhedra of Clar type. *J. Chem. Soc., Faraday Trans.* **1994**, *90*, 2865−2871.

(16) Diudea, M. V. Capra−a leapfrog related operation on maps. *Stud. Univ. Babes−Bolyai, Chem.* **2003**, *48* (2), 3−16.

(17) Diudea, M. V. Covering forms of nanostructures. *Forma* **2004**, in press.

(18) Diudea, M. V. Covering nanostructures. In *Nanostructures−Novel Architecture*; NOVA: New York, in press.

(19) Goldberg, M. A class of multi-symmetric polyhedra. *Tôhoku Math. J.* **1937**, *43*, 104−108.

(20) Nagy, C. L.; Diudea, M. V. Nanoporous carbon structures. In *Nanostructures-Novel Architecture;* Diudea, M. V., Ed.; NOVA: New York, in press.

(21) Nagy, C. L.; Diudea, M. V. Carbon allotropes with negative curvature. *Stud. Univ. Babes−Bolyai, Chem.* **2003**, *48* (2), 37−46.

(22) Mackay, A. L.; Terrones, H. Diamond from graphite. *Nature* **1991**, *352*, 762−762.

(23) Vanderbilt, D.; Tersoff, J. Negative-curvature fullerene analogue of C_{60}. *Phys. Rev. Lett.* **1992**, *68*, 511−513.

(24) Lenosky, T.; Gonze, X.; Teter, M.; Elser, V. Energetics of negatively curved graphitic carbon. *Nature* **1992**, *355*, 333−335.

(25) El-Basil, S. Combinatorial self-similarity. *Croat. Chem. Acta* **1996**, *69*, 1117−1148.

(26) Klein, D. J.; Živković, T. P.; Balaban, A. T. The fractal family of coro(n)enes. *MATCH* **1993**, *29*, 107−130.

(27) Harary, F. *Graph Theory*; Addison-Wesley: Reading, MA, 1969.

(28) Gross, J. L.; Tucker, T. W. *Topological graph theory*; Dover Publications: Mineola, NY, 2001.

(29) Klein, D. J. Topo-graphs, embeddings, and molecular structure. In *Chemical topology*; Bonchev, D., Rouvray, D. H., Eds.; Gordon & Breach: Amsterdam, 1999; pp. 39−83.

(30) Hyde, S. T. Sponges, Foams and Emulsions. In *Foams and Emulsions*; Sadoc, J. F., Rivier, N., Eds.; Kluwer: Dordrecht, The Netherlands, 1999; NATO ASI Series E: Applied Sciences, Vol. 354, pp. 437−469.

(31) Haddon, R. C. Rehybridization and π-orbital overlap in nonplanar conjugated organic molecules: π-orbital axis vector (POAV) analysis and three-dimensional Hückel Molecular Orbital (3D-HMO) theory. *J. Am. Chem. Soc.* **1987**, *109*, 1676−1685.

(32) Haddon, R. C. Measure of nonplanarity in conjugated organic molecules: which structurally characterized molecule displays the highest degree of pyramidalization? *J. Am. Chem. Soc.* **1990**, *112*, 3385−3389.

(33) Haddon, R. C. C_{60}: sphere or polyhedron? *J. Am. Chem. Soc.* **1997**, *119* (9), 1797−1798.

(34) Haddon, R. C.; Chow, S.-Y. Hybridization as a metric for the reaction coordinate of chemical reactions. *J. Am. Chem. Soc.* **1998**, *120*, 10494−10496.

(35) Terrones, H.; Mackay, A. L. Triply periodic minimal surfaces decorated with curved graphite. *Chem. Phys. Lett.* **1993**, *207*, 45−50.

(36) Valencia, F.; Romero, A. H.; Hernàndez, E.; Terrones, M.; Terrones, H. Theoretical characterization of several models of nanoporous carbon. *New J. Phys.* **2003**, *5*, 123.1−123.16.

(37) Terrones, H.; Terrones, M. Curved nanostructured materials. *New J. Phys.* **2003**, *5*, 126.1−126.37.

(38) Schwarz, H. A. Über Minimalflächen. *Monatsber. K. Akad. Wiss. Berlin* **1865**.

(39) Schwarz, H. A. *Gesammelte Matematische Abhandlungen*; Springer: Berlin, 1890.

(40) Karcher, H.; Polthier, K. Construction of triply periodic minimal surfaces. *Philos. Trans. R. Soc. London, Ser. A* **1996**, *354*, 2077−2104.

(41) Terrones, H.; Mackay, A. L. From C_{60} to negatively curved graphite. *Prog. Cryst. Growth Charact.* **1997**, *34*, 25−36.

(42) O'Keeffe, M.; Adams, G. B.; Sankey, O. F. Predicted new low energy forms of carbon. *Phys. Rev. Lett.* **1992**, *68*, 2325−2328.

(43) Terrones, H.; Terrones, M. Fullerenes and nanotubes with nonpositive Gaussian curvature. *Carbon* **1998**, *36*, 725−730.
(44) Diudea, M. V.; Stefu, M.; John, P. E.; Graovac, A. Generalized operations on maps. *Croat. Chem. Acta* **2005**, submitted.
(45) Rodriguez-Manzo, J.-A., Lopez-Urias, F., Terrones, M., Terrones, H. Magnetism in corrugated carbon nanotori: The importance of symmetry, defects and negative curvature. *Nanoletters* **2004**, *4*, 2179−2183.
(46) Klein, F. *Vorlesungen ber das Ikosaede;* Teubner: Leipzig, Germany, 1884; Part I, Chapter II.
(47) Klein, F. *Gesammelten Mathematischen Abhandlungen*; Springer-Verlag: Berlin, 1923; Vol. 3, pp 90−136.
(48) Ceulemans, A.; King, R. B.; Bovin, S. A.; Rogers, K. M.; Troisi, A.; Fowler, P. W. The heptakisoctahedral group and its relevance to carbon allotropes with negative curvature. *J. Math. Chem.* **1999**, *26*, 101−123.
(49) Terrones, M.; Banhart, F.; Grobert, N.; Charlier, J.-C.; Terrones, H.; Ajayan, P. M. Molecular junctions by joining single-walled carbon nanotubes. *Phys. Rev. Lett.* **2002**, *89*, 075505-1−075505-4.
(50) Stefu, M.; Diudea, M. V. *CageVersatile*, version 1.5; Babes−Bolyai University: Cluj, Romania, 2005.

CI050054Y